Interpixel capacitance in large format CMOS hybrid arrays

G. Finger *, R. Dorn, M. Meyer, L. Mehrgan,
A.F.M. Moorwood and J. Stegmeier
European Southern Observatory, Karl Schwarzschildstr.2, D-85748 Garching, Germany

ABSTRACT

Since adaptive optics on large telescopes provides almost diffraction limited resolution, Nyquist sampling of moderate fields requires large format arrays. Because of limited substrate sizes there is a tendency to shrink the pixel size to extend the array format beyond 2Kx2K. However, with smaller pixel sizes the coupling capacitance between neighboring pixels becomes more important and its effect on performance and basic parameters of large format arrays has to be analyzed. Therefore, techniques to measure the effect of the coupling capacitance on the conversion gain will be presented. The capacitance comparison method and the autocorrelation technique will be discussed and compared quantitatively. It will be shown that the "noise squared versus signal" method which is in common use to obtain the conversion gain, can only be applied for negligible interpixel capacitance. The X-ray decay of Fe55 is a well established calibrator for silicon and can be applied to Si-PIN diode arrays in order to verify the different methods. Finally, a new technique called single pixel reset will be presented, which directly measures the impulse response or point spread function generated by the inter-pixel capacitance. The measured PSF impulse response can be used for the deconvolution of images to compensate the degradation of spatial resolution induced by the interpixel capacitance. The difference of interpixel capacitance measured in infrared hybrid arrays and Si-PIN diode arrays hybridized to the same multiplexer will be discussed.

Keywords:, interpixel capacitance, conversion gain, point spread function, single pixel reset, CMOS hybrid, Hawaii-2RG, HgCdTe, Si-PIN, HyViSI

1. INTRODUCTION

A basic parameter characterizing the performance of CMOS hybrid active pixel sensors is the conversion gain C_0/e measured in units of electrons per Volt. C_0 is the nodal capacitance of the integrating node of the detector pixel. All other parameters such as readout noise, dark current and quantum efficiency depend on the accurate determination of the conversion gain. Since the measurement of the quantum efficiency of a λ_c=2.5µm HgCdTe Hawaii-2RG array lead to inconsistent results with quantum efficiencies exceeding 100%, we tried to narrow down the errors of all factors influencing the quantum efficiency such as the radiation geometry, the blackbody calibration, the temperature dependence of the filter transmission, radiation leaks of filters, etc [1]. However, it was not possible to obtain a quantum efficiency in K-band below 105%. For Si-PIN diode arrays hybridized to the same Hawaii-2RG multiplexer the measured quantum efficiency was 200%. The remaining major uncertainty is the conversion gain C_0/e. The nodal capacitance C_0 is composed of the voltage dependent diode capacitance of the detector pixel and the fixed gate capacitance of the unit cell source follower gate. It is usually determined by the widely used shot noise method assuming photon shot noise limited performance of the detector. Photons are governed by Poisson statistics with the variance of the integrated number of photons equal to the mean number of photons. For this case, the nodal capacitance C_0 can be calculated from the slope of the plot of "noise squared versus mean" signal according to Eq. (1). However, this equation only holds true if the signals of neighbouring pixels are uncorrelated as explained in section 6.

$$C_0 = e\frac{\langle V \rangle}{\langle V^2 \rangle} \tag{1}$$

Measurements on the Si-PIN array were made on a single engineering device whereas measurements on HgCdTe arrays have been carried out with different devices in the course of the evaluation of detectors for the Hawk-I mosaic. The conversion gain may vary by < 20% for different devices.

*gfinger@eso.org; phone +49-89-32006256; fax +49-89-3202362; www.eso.org/~gfinger

2. CONVERSION GAIN BY CAPACITANCE COMPARISON

In order to obtain the nodal capacitance C_0 by a direct measurement which does not rely on statistical methods, a simple technique has been developed which is described in more detail in [1]. It is based on comparing the voltage change of a large calibrated external capacitor to that of the unknown nodal capacitance C_0 which is many orders of magnitude smaller. During normal operation the reset voltage V_{reset} is connected to an external bias voltage of the detector control electronics and the bias provides the charge required to reset the integrating node capacitor. The hardware setup for the capacitance comparison simply entails adding a switch (relay) between the bias and V_{reset} and adding a calibrated capacitor between V_{reset} and detector substrate voltage D_{sub} as shown in Figure 7. The external capacitor is then charged to the nominal reset voltage and disconnected (using the relay) from the external bias. The charge to reset the nodal capacitor C_0 of each pixel slowly discharges the external capacitor, C_{ext}.

$$\Delta V_{ext} C_{ext} = \sum_{n=1}^{n_{frames}} \sum_{i=1}^{2048} \sum_{j=1}^{2048} V_{n,i,j} C_0 \qquad (2)$$

If the 2Kx2K pixels of the detector are exposed to a high photon flux and several frames are read out and reset, the charge to repeatedly reset the complete array will discharge C_{ext} sufficiently to generate a voltage drop ΔV_{ext} across C_{ext} large enough to be accurately measured.

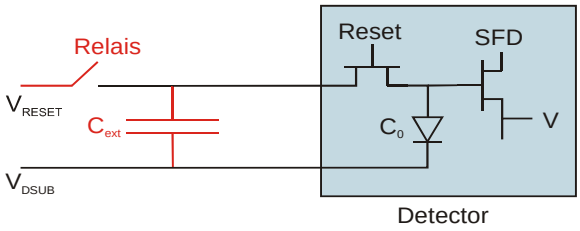

Figure 1 Hardware setup of capacitance comparison method for the measurement of the conversion gain

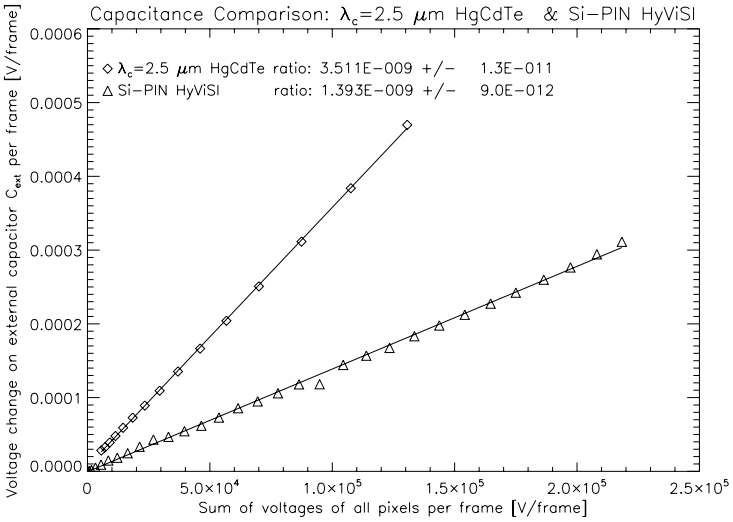

Figure 2 Voltage drop across the external capacitor Vext versus the sum of the voltages of all detector pixels (total detector signal) for the corresponding flux level. The total detector signal is changed by increasing the photon flux on the detector. The slope of the least square fit is the ratio of the nodal capacitance and the external capacitance C0/Cext .

Deleted:

Since the voltage drop ΔV_{ext} on C_{ext} and the signals of each pixel $V_{i,j}$ are known, the nodal capacitance C_0 and thus the conversion gain C_0/e can be calculated using Eq. (2). The voltage drop ΔV_{ext} and the total integrated detector signal have been measured at different flux levels as shown in Figure 2. The slope of the plot is the ratio of nodal capacitance C_0 and the external capacitance C_{ext} . A capacitance of 9.79 μF was used for C_{ext}. It is much larger than the sum of the capacitance of all cables and other stray capacitances. The capacitances of these components may therefore be neglected. The discrepancy of nodal capacitances C_0 determined by the capacitance comparison and the shot noise method is substantial (> 10% for HgCdTe and more than a factor of two for Si-PIN arrays) as can be seen in Table 1. Nodal capacitances obtained with the capacitance comparison method (Table 1) yield a quantum efficiency for the HgCdTe Hawaii-2RG array in K-band of 86% and for the Si-PIN Hawaii-2RG array at 650 nm of 95% [2]. Plausible quantum efficiencies cannot be obtained with conversion gains derived from the standard "noise squared versus signal" technique.

The capacitance comparison method is a powerful technique to measure the voltage dependence of the nodal capacitance. Since the depletion width of the pn junction of the detector diode decreases with decreasing reverse bias voltage, the capacitance and the corresponding conversion gain C_0/e increase as well, and is becoming the main contribution to the nonlinearity of CMOS arrays with source-follower inputs. The nodal capacitance C_0 is the sum of the fixed gate capacitance of input FET of the unit cell C_g and the voltage dependent junction capacitance of the detector diode C_d. The voltage dependence is given by equation (3) below:

$$C_0 = C_G + C_D \quad with \quad C_D(V) = \sqrt{\frac{e\varepsilon\varepsilon_0}{2(V_{BI} + V_{DSUB} - V_{RESET})} \frac{N_A N_D}{N_A + N_D}} \tag{3}$$

In equation (3) V_{BI} is the built in potential of the junction, N_D and N_A are the concentration of donors and acceptors and ε is the static dielectric constant of λ_c=2.5μm HgCdTe which is 14.67. The nodal capacitance measured on a HgCdTe array with the capacitance comparison method is represented by diamonds in Figure 3 and plotted versus the detector substrate voltage V_{DSUB}.

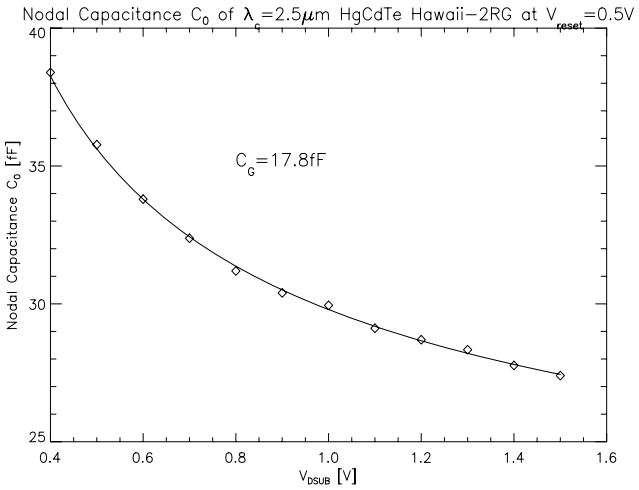

Figure 3 Nodal capacitance C_0 as function of detector substrate voltage V_{DSUB}. The reverse bias voltage is V_{DSUB}- V_{RESET} with V_{RESET} set to V_{RESET} =0.5 V.

The solid line in Figure 3 is derived from a linear fit of measured values of C_D, which are plotted as $1/(C_D)^2$ versus reverse bias voltage V_{RESET} -V_{DSUB} as shown in Figure 4. The capacitance of the unit cell source follower gate C_G was determined by maximizing the linear correlation coefficient of this fit yielding a value of C_G = 17.8 fF. This gate capacitance is quite large for a nodal capacitance of C_0=27.3 fF. Since the junction capacitance of the detector diode is only C_D=9.5 fF it may be considered in future multiplexer designs to reduce the gate capacitance C_G to ~ 10 fF to reduce the overall conversion gain and improve the noise performance of the detector at the expense of somewhat reduced linearity.

From the slope of the plot in Figure 4 the doping concentration of the detector can be deduced. Since the HgCdTe diodes of the Hawaii-2RG array are p^+-n diodes, the acceptor concentration $N_A >> N_D$. Using equation (3) the donor concentration can be shown to be proportional to the inverse slope of the $1/C_D^2$ versus bias plot, which is shown in Figure 4. The relation between the donor concentration N_D and the slope of Figure 4 is given by equation (4):

$$N_D = -\frac{2}{e\varepsilon\varepsilon_0}\frac{1}{d(1/C_D^{\,2})/dV} \quad if \quad N_A >> N_D \tag{4}$$

The donor concentration is kept as low as possible to still make reliable arrays. The value obtained from our $C_0(V)$ measurement is 1.2 10^{14} cm^{-3}. The built in potential V_{BI} is just the intercept of the $1/(C_D)^2$ plot with the axis of the bias voltage. It is V_{BI} = 412 mV.

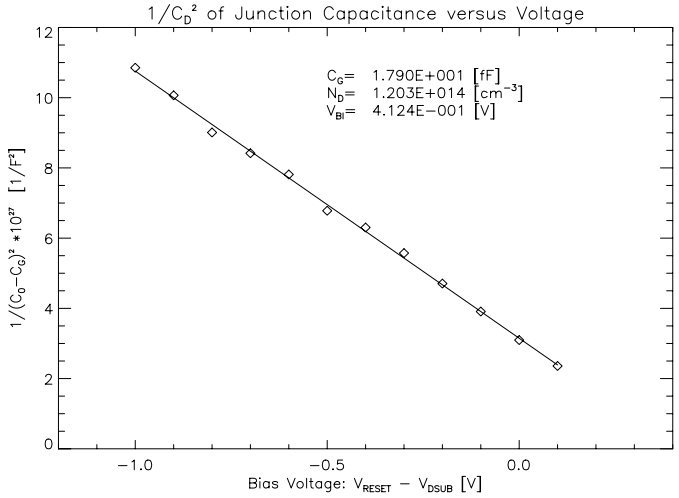

Figure 4 $1/C_D^2$ plot versus bias voltage V_{RESET} -V_{DSUB}. C_G was determined by maximizing the linear correlation coefficient.

With the parameters extracted from the $C_0(V)$ measurement it is possible to build an accurate model of the detector diode based on measured parameters which allow to predict the signal response and the non-linearity of the detector.

3. CONVERSION GAIN BY FE55

In an effort to compare and validate the two methods of deriving the conversion gain, namely the "noise squared versus signal" and the capacitance comparison method, we used the K_α line of Fe^{55} which generates a well known number of electrons per absorbed x-ray photon and has been in use for many years to calibrate the conversion gain of optical CCD's [3]. Unfortunately, the Fe^{55} method cannot be applied to the HgCdTe arrays because the CdZnTe substrate absorbs the x-rays of the Fe^{55} source before they reach the depletion region of the infrared diodes. For the Si-PIN diode array, however, the Fe^{55} calibration is applicable. A histogram showing the number of electrons generated by the absorption of one X-ray photon is shown in Figure 5. The solid curve represents the histogram generated by using the nodal capacitance C_0 determined by the capacitance comparison method; the dashed curve shows the histogram of the same data set but using the nodal capacitance determined by the standard photon transfer curve (shot noise) technique. The accepted value used in calibrating CCD's is shown as a vertical line in Figure 8. It is evident that the capacitance comparison method is consistent with the Fe^{55} value cited in the literature. The shot noise method using "noise squared versus signal" can only be applied if the coupling between pixels due to the interpixel capacitance can be neglected as explained in the next section.

The Fe^{55} method can also be applied to InSb detectors which do not have a detector substrate. First measurements yield a value of 2500 electrons per absorbed K_α x-ray photon. Possibly, the Fe^{55} method will also be applicable to HgCdTe arrays, if their substrates are removed. Further measurements are planned, when we will receive substrate removed HgCdTe arrays.

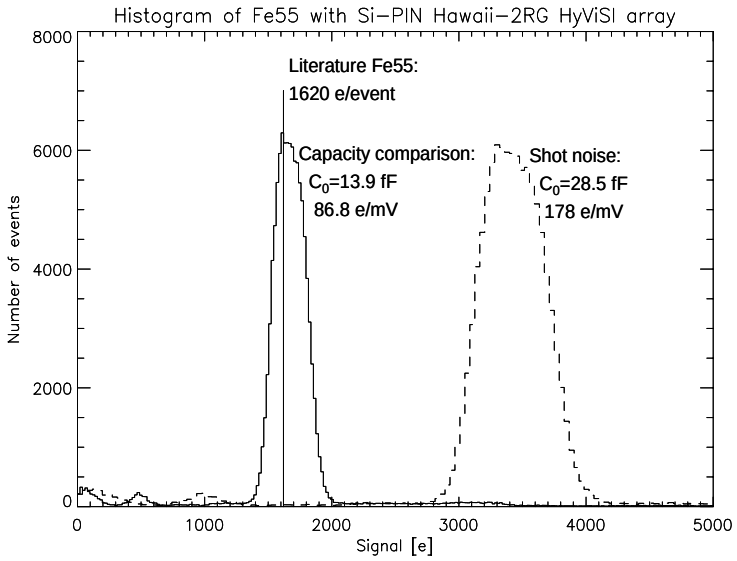

Figure 5 Histogram of Hawaii-2RG Si-PIN HyViSI array exposed to Fe55 X-ray source. The same data set is plotted with nodal capacitances derived from capacitance comparison method (solid histogram) and the shot noise method (dashed histogram). Literature value is indicated as a vertical line.

4. CONVERSION GAIN AND INTERPIXEL CAPACITANCE

The nodal capacitance C_0 derived with the shot noise method appears to be too large. Since Eq. (1) shows that C_0 is inversely proportional to the variance, the measured variance of the detector signal $\langle V^2 \rangle$ should be larger to obtain a smaller but more plausible nodal capacitance, i.e., the shot noise method appears to have too low a signal variance. The discrepancy cannot be explained by excess noise of the data acquisition chain as more noise would only make the variance larger not smaller. On the contrary, a mechanism has to be introduced which does not change the signal charge but reduces the photon shot noise of a single pixel. The larger capacitance seen by the shot noise may be explained by coupling capacitance between neighboring pixels. As a consequence of the interpixel capacitances the signal of the pixel which is hit by a photon is spread by capacitive coupling to adjacent pixels, which reduce the apparent photon shot noise. While the mean signal remains unchanged the variations about the mean are "smoothed" by the capacitive coupling to neighboring pixels. Hence, the photon shot noise method does not yield the pixel capacitance C_0, but the sum of C_0 and all the coupling capacitors in series with the nodal capacitors of the neighboring pixels as shown in Figure 6. Using the coupling capacitance C_c and the ratio of coupling capacitance and nodal capacitance $x = C_c/C_0$, a simple model of the apparent capacitance C seen by the shot noise is $C = C_0(5x+1)/(x+1)$. For simplicity, only coupling to the 4 closest neighbors is considered here. By applying Kirchhoff's laws it can also be shown, that the total signal with coupling V_0+4V_i is equal to the total signal V without coupling, i.e., $V_0+4V_i = V$ with V the signal for $C_c=0$. This implies that the interpixel capacitive coupling conserves photometry. For uniform illumination of the array no signal charge is stored on the coupling capacitors. The coupling capacitors reduce the photon shot noise because the voltage response of

a photon-generated electron is not confined to a single pixel, but spread over all neighboring pixels. This nominal reduction of noise is accompanied by reduced image contrast and degraded detector MTF.

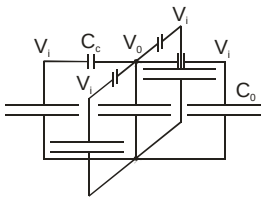

Figure 6 Interpixel coupling capacitance. Only next neighbors are considered.

The coupling capacitance C_c in Si-PIN diode arrays is much larger than in HgCdTe infrared arrays. The reason for the difference is the fact, that the detector bulk of Si-PIN diodes is fully depleted, whereas in HgCdTe arrays each pixel diode maintains its own local depletion region as shown in Figure 7. Shaded areas in Figure 7 are equipotential areas, either neutral p or n regions or In bumps between the diode array and the Si multiplexer. Adjacent pixels of HgCdTe arrays are separated by the n-doped bulk of HgCdTe which is conducting and surrounds the pixel. Since no electric field can build up between pixels, they are screened from each other. The n-doped bulk acts as a guard ring screening neighboring pixels from capacitive coupling. Capacitive coupling can only occur in the space between the infrared array and the Si multiplexer between the In-bumps and to some extent also within the multiplexer itself. In the Si-PIN diode array of the HyViSI detector the bulk of the silicon is fully depleted and the electric fields can also build up between pixels resulting in the large observed interpixel capacitance. Since the Si-PIN HyViSI array uses similar In bumps and exactly the same multiplexer as the HgCdTe array, but exhibits much stronger interpixel coupling, it may be assumed that the main coupling occurs inside the Si-PIN diode array. The coupling can be reduced by reducing the size of the p implants, which increases the separation between the conducting p regions and decreases the coupling capacitance between adjacent pixels. The coupling capacitance C_c does not depend on the applied bias voltage DSUB or VSUB, since these voltages only change the electric field normal to the array surface and have no effect on the electric field parallel to the surface in the direction of the interpixel coupling.

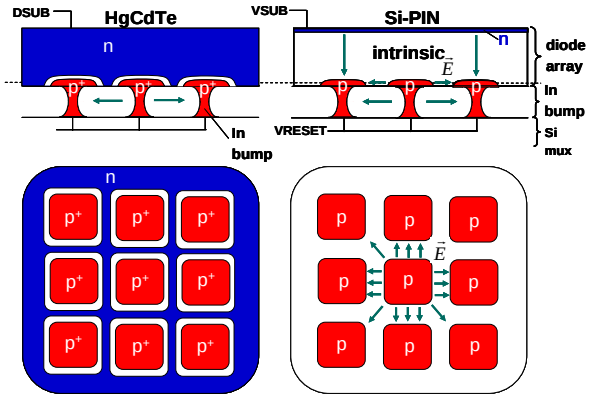

Figure 7 Structure of HgCdTe (left) and Si-PIN diode arrays. White area is free of charge carriers with electric field between pixels. Shaded areas are p or n regions with freely movable charge carriers. Depletion regions of neighboring pixels in HgCdTe arrays are separated by conducting n bulk of detector. The bulk of Si-PIN arrays is fully depleted with capacitive coupling between pixels inside diode array.

5. MEASUREMENT OF INTERPIXEL CAPACITANCE POINT SPREAD FUNCTION

The Hawaii-2RG multiplexer has a unique feature, the guide mode, which is implemented for telescope guiding and correction of fast image motion induced by atmospheric turbulence. The guide mode operation allows simultaneous

operation of the full array read out at a frame rate of 1 Hz and a small sub-window read out at frame rates of a few hundred Hz. Since the reset of the small guide window can be controlled independently from the full frame, this feature makes it possible to determine in a very direct way the impulse response or the point spread function (PSF) generated by capacitive coupling between adjacent pixels [4]. If the size of the guide window is reduced to a single pixel which is reset at a much higher frequency than the full 2Kx2K array, which is uniformly illuminated, the integration time for the guide window pixel is much shorter than for the full array. Consequently, the signal of the guide window pixel will be almost zero, whereas all other pixels will have integrated a large number of photon generated charges. Using the annotation of Figure 6 and assuming the guide window pixel is the central pixel, the voltage V_0 of the guide window pixel will be almost zero and the voltage for all other pixels will be large and uniform, except for the pixels very close to the guide window pixel. Depending on the ratio of the coupling capacitance C_c and the nodal capacitance C_0, the capacitive voltage division will slightly reduce the signal of the neighbors surrounding the guide window pixel. The normalized difference of two images, one taken with the reset of the guide window pixel switched on and one taken without resetting the guide window pixel, directly yields the point spread function generated by the capacitive coupling of the interpixel capacitance. The single pixel reset measurement is also sensitive to the readout speed. Enough settling time has to be given to the video signal. In our experiment the detector was operated at a frame rate of 0.59Hz.

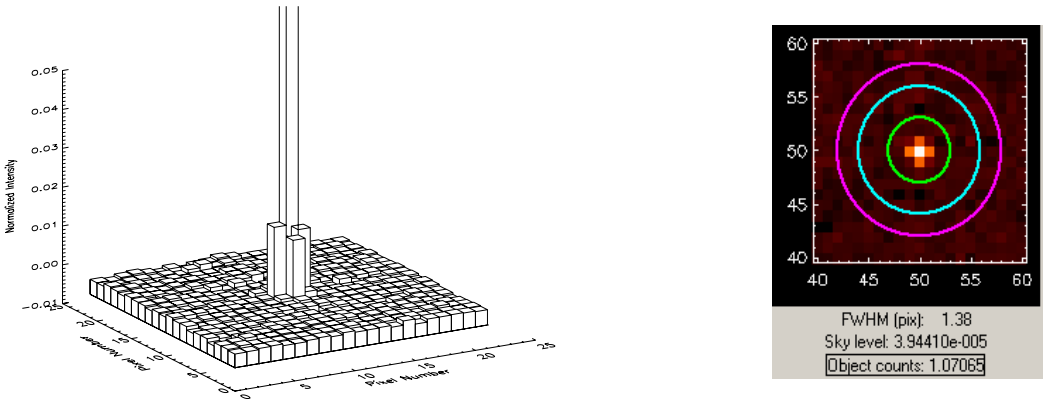

Figure 8 Normalized point spread function of interpixel capacitance of HgCdTe Hawaii-2RG array measured by single pixel reset using the guide window mode. Intensity of closest neighbors: upper 1.4%, lower 1.5%, left 1.8%, right 1.7%. Total integrated intensity 1.07.

The point spread function (PSF) shown as surface plot in Figure 8 is normalized to the intensity of the central pixel. The interpixel coupling of the HgCdTe array spills ~ 1.75 % of the central pixel intensity to the neighboring pixels in the fast readout direction and ~ 1.45% to neighbors in the slow readout direction. On other HgCdTe Hawaii-2RG arrays large coupling of 2.5 % has been observed. If the normalized PSF is divided by the integrated PSF which has an area of 1.07 the impulse response function of capacitive coupling is obtained. The normalized PSF of capacitive coupling for both HgCdTe and Si-PIN Hawaii-2RG arrays can be downloaded from the author's web page [5] for further modeling.

In Figure 9 the PSF of the Si-PIN Hawaii-2RG array is shown. The signal coupled to the closest neighbors is upper 8.5% in the slow and 9.3% in the fast readout direction. The total integrated intensity is 1.74, the value by which the normalized PSF has to be divided to obtain the impulse response.

The measurement of the Si-PIN H2RG PSF obtained with the single pixel reset yields almost identical results as the optical PSF measured by Dorn et al.[2]. The optical PSF is composed of all contributions, the capacitive coupling between pixels as well as charge diffusion and optical crosstalk. The optical PSF measurement shows, that capacitive coupling between neighboring pixels is the dominant contribution to the detector PSF.

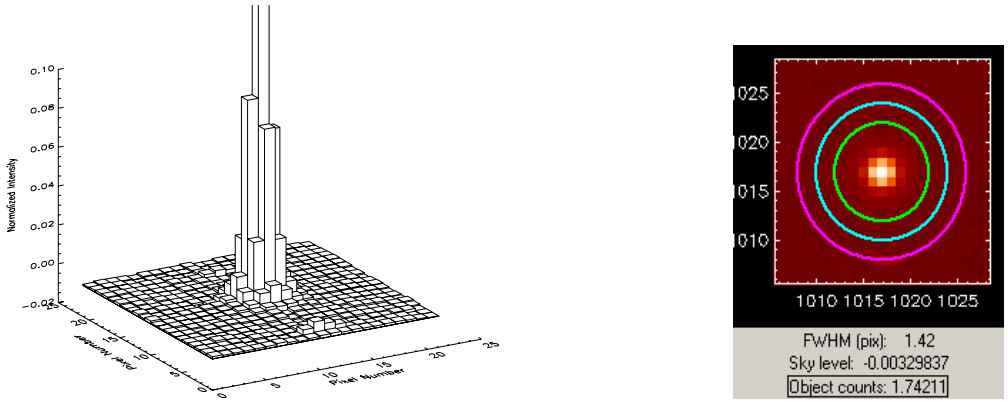

Figure 9 Normalized point spread function of interpixel capacitance of Si-PIN Hawaii-2RG array measured by single pixel reset using the guide window mode. Intensity of closest neighbors: upper 8.2%, lower 8.8%, left 10.2%, right 8.45%. Total integrated intensity 1.74.

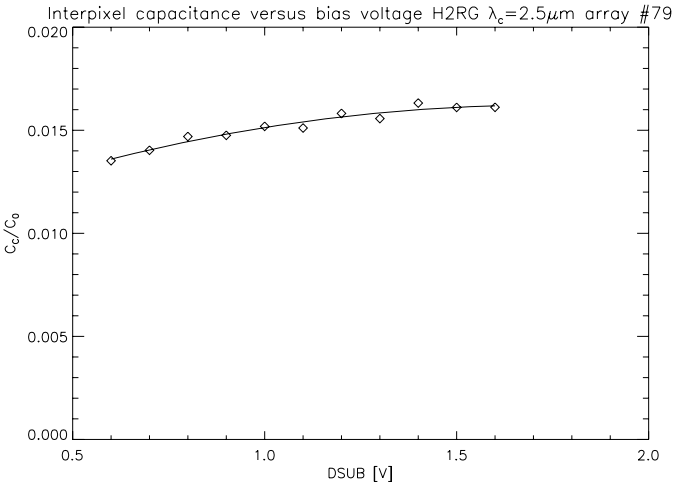

Figure 10 Normalized interpixel capacitance C_c/C_0 versus bias voltage for HgCdTe array. Increase of Cc/C_0 is due to decrease of C_0 with increasing bias DSUB. C_c does not depend on DSUB.

For the HgCdTe array the dependence of the coupling capacitance C_C on the bias voltage is shown in Figure 10. The normalized coupling capacitance C_C/C_0 was determined from the ratio of the average signal of the 4 next neighbors and the central pixel of a single pixel reset image measured at different substrate voltages. The increase of Cc/C_0 is due to decrease of C_0 with increasing detector bias DSUB. As expected, the coupling capacitance C_c does not depend on DSUB, since the coupling occurs between the In bumps and on the multiplexer.

6. AUTOCORRELATION

A. Moore et al. have examined the detector edge spread and MTF; they were the first to introduce interpixel coupling as one mechanism to degrade the image sharpness of CMOS hybrid detectors [6]. Moore devised a stochastic method of measuring the interpixel coupling using 2D autocorrelation, which is briefly outlined in Figure 11. The capacitive coupling between pixels can be regarded as a system degrading the performance of an image similar to an imperfect

optical system characterized by the point spread function PSF. The PSF is the impulse response $h(\vec{x})$ of the system as shown on the left side of Figure 11. The impulse response can be measured with the single pixel reset method described above. Because of Poisson statistics, in the frequency domain the variance of the difference of two images taken with the array being uniformly illuminated is 2N, with N being the number of photons per pixel. The power spectral density PSD at the input of the system is white and equals 2N. The factor of 2 is expressing the fact, that the difference of 2 uncorrelated images is used. $\vec{\xi}$ is the vector of spatial frequency. Since the transfer function of the system in the frequency domain $H(\vec{\xi})$ is the Fourier transform of the impulse response $FT(h(\vec{x}))$, the PSD at the output of the system is $2N\left|H(\vec{\xi})\right|^2$. The Wiener Kinchine theorem states that the Fourier transform of the Autocorrelation function $A(\vec{x})$ is equal to the PSD as shown in equation (3)

$$2N\left|H(\vec{\xi})\right|^2 = FT(A(\vec{x})) \tag{3}$$

Instead of working in the frequency domain the Wiener Kinchine theorem allows returning to the spatial domain and apply autocorrelation techniques. Taking the inverse Fourier transform and integrating equation (3) in the spatial domain yields the result of equation (4), since the impulse response and the convolution of the impulse response with itself is unity.

$$\int A(\vec{x})d\vec{x} = 2N \tag{4}$$

Moore's important result is that the "noise squared versus signal" method overestimates the nodal capacitance [6]. The method can still be applied if the integrated autocorrelation is used instead of the Autocorrelation at 0, which is equal to the variance. The discrete form of equation (4) is given in equation (5) with α being the conversion gain in e/V, n_{pix} the number of pixels used for the summation over i,j, $D_{i,j}$ the voltage of the difference of two uniform flat fields, and V the mean signal voltage of the flatfield.

$$\sum_{m,n} A_{m,n} = \frac{\alpha^2}{n_{pix}} \sum_{m,n}\sum_{i,j} D_{i,j}D_{i+m,j+n} = 2N = 2\alpha V \quad with \quad \alpha = \frac{C_0}{e} \tag{5}$$

If all the cross products $D_{i,j}D_{i+m,j+n}$ with $m \neq 0$ and $n \neq 0$ are 0, the signals of neighboring pixels are not correlated, since the interpixel capacitance is negligible. For this case the sum in equation (5) is the variance and the "noise squared versus signal" method yields the correct nodal capacitance. If there is a correlation between neighboring pixels due to coupling capacitances, the correct nodal capacitance can still be derived from the shot noise of difference images by properly taking the correlation between pixels into account and using the full sum of equation (5) which is the discrete form of the integrated autocorrelation function of equation (4).

The autocorrelation function was measured by uniformly illuminating the array with a stable radiation source. For the HgCdTe array an extended blackbody was put in front of the entrance window of the dewar. Only a stripe of 256x2048 pixels was read out using double correlated sampling to reduce the detector integration time to 205 ms, thus avoiding thermal drifts and low frequency pickup. Since 32 outputs have been used, even for the short integration time of 205 ms the pixel time was as long as 12 μs, which is sufficiently large to minimize the electrical crosstalk in the fast readout direction due to the limited bandwidth of the analog video signal processing chain of the multiplexer and the readout electronics. This is critical, since electrical crosstalk generates correlation in the fast readout direction and would mask correlation due to capacitive interpixel coupling. A cosmetically clean region in the selected stripe was chosen to calculate the autocorrelation function from the difference of subsequent images.

The integrated autocorrelation divided by the variance is the factor φ by which the nodal capacitance is overestimated if the variance is used for the "noise squared versus signal" method. We determined the correction factors φ for both devices, the HgCdTe and the Si-PIN Hawaii-2RG array. The measured values are φ_{HgCdTe}=1.10 for the HgCdTe array and $\varphi_{Si\text{-}PIN}$=1.97 for the HyViSI Si-PIN array. Both arrays are hybridized to the same type of Hawaii-2RG multiplexers.

Correlation between neighboring pixels for the HgCdTe array can only be observed for the next neighbors, whereas the correlation of Si-PIN array extends over three pixels in each direction.

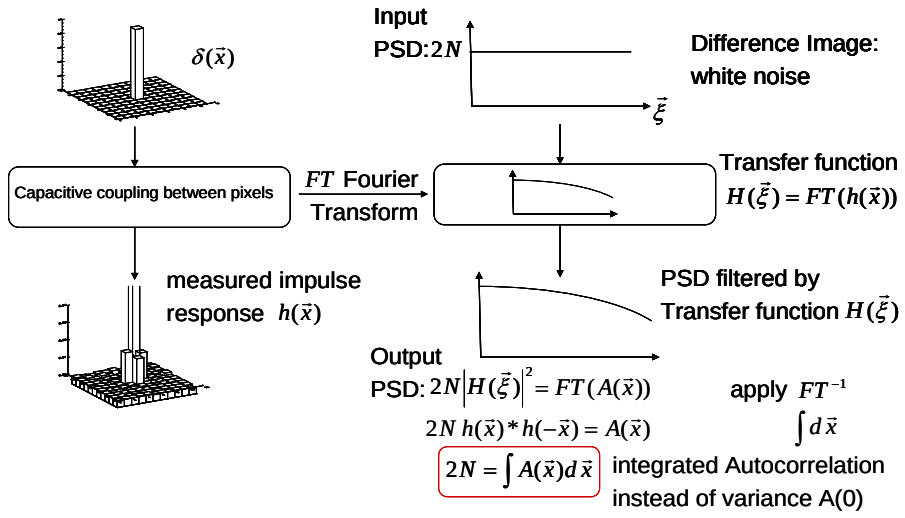

Figure 11 Derivation of stochastic method to determine conversion gain. Instead of the variance A(0) the integrated autocorrelation has to be applied for the "noise squared versus signal" method to measure the conversion gain.

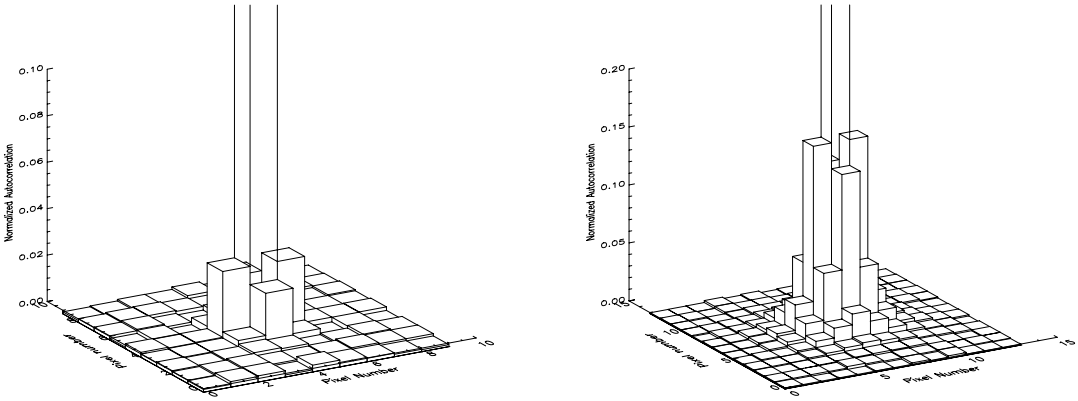

Figure 12 Normalized autocorrelation. Left: HdCdTe Hawaii-2RG array. φ=1.10 Right: Si-PIN Hawaii-2RG array. φ=1.97.

To convert the measured ADC units to volts at the integrating node of the detector, the gain of the readout electronics has to be calibrated. By keeping both the high and the low voltage of the reset clock high, the reset switch is permanently closed. The reset voltage Vreset is then varied and the output of the detector signal is plotted in ADU units versus the reset voltage. From the slope of the measured curve shown in Figure 13 one can obtain the electronic gain in ADU/V , with V being the voltage at the anode side of the detector diode. The same measurement can be carried out varying the reference voltage at the input of the cryogenic preamplifiers. The ratio of the gains is the gain of the two stages of the on-chip detector source followers from the unit cell to the detector output. The overall detector source follower gain is 0.97, which is a big improvement in comparison to previous detectors (Hawaii1 1Kx1K).

In order to measure the integrated autocorrelation as a function of flux on the detector, the temperature of a blackbody was varied from 50°C to 120°C in steps of 2C. For each temperature 16 difference images were taken in H-band and the average autocorrelation function from these differences was calculated. The plot is shown in Figure 14 and represented by diamonds. The autocorrelation has to be divided by 2, because the difference of two images is used.

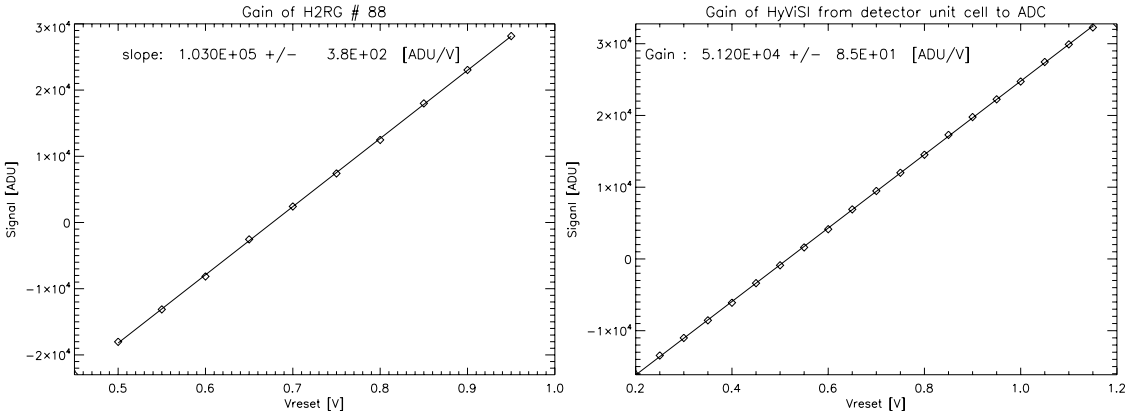

Figure 13 Electronic gain of HgCdTe Hawaii-2RG array (left Figure) and Si-PIN HyViSI array (right Figure) measured from detector unit cell to ADC input of data acquisition system.

The inverse slope of the obtained plot is the conversion gain in V/e. The autocorrelation at zero, which is the variance, is represented by triangles in Figure 14 and represents the classical "noise squared versus variance" method to obtain the conversion gain. For the Si-PIN array the same procedure was applied replacing the blackbody by a light emitting diode and an Ulbricht sphere which illuminates the detector. The inverse slope of the integrated autocorrelation versus the mean signal is the conversion gain in e/V.

For the HgCdTe array the integrated autocorrelation yields a conversion gain of 228 e/mV and the autocorrelation at zero which is equal to the variance yields a gain of 251 e/mV. The "noise squared versus variance" method overestimates the conversion gain by 10 % because it does not take into account the correlation between pixels induced by capacitive coupling. This discrepancy is much larger in Si-PIN diode arrays. The integrated autocorrelation yields a conversion gain of 86 e/mV, whereas the variance yields a gain of 170 e/mV which is too high by a factor of two. If neighboring pixels are correlated by capacitive coupling, the variance cannot be used as an estimator for the photon shot noise but hast to be replaced by the integrated autocorrelation.

In table 1 the values of the conversion gain obtained with the integrated autocorrelation method are compared with the values deduced with the capacitance comparison method and the Fe55 method. The quantitative agreement is within the experimental uncertainty. The external capacitance was measured to be 9.79μF. The quantitative agreement is within the experimental uncertainty.

Table 1 Comparison of conversion gains C_0/e and nodal capacitances C_0 of CMOS hybrid arrays determined by shot noise , integrated autocorrelation, capacitance comparison and Fe^{55} method

Method	Noise squared versus signal	Integrated Autocorrelation	Capacitance comparison	Fe^{55}
HgCdTe HRG #88				
C_o/e [e/mV]	251.3	227.6	215	
C_o [fF]	40.3	36.4	34.5	
Si-PIN HyViSI				
C_o/e [e/mV]	170.0	86.3	85.1	86.8
C_o [fF]	27	13.8	13.6	13.9

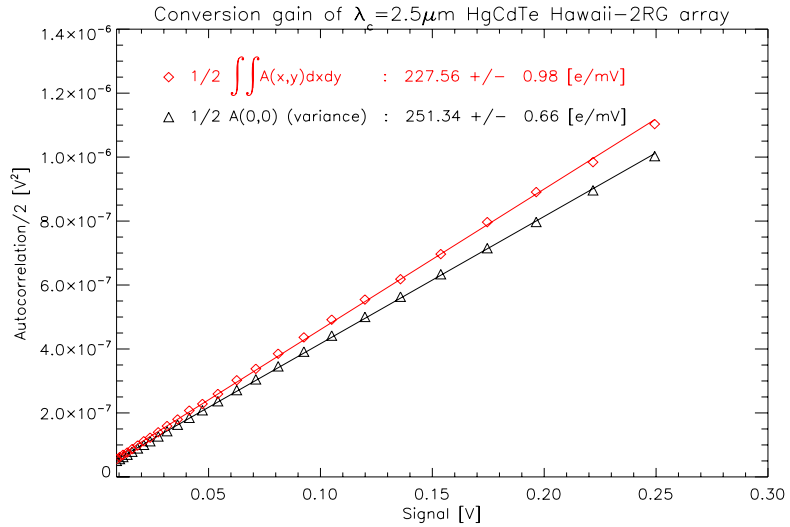

Figure 14 Conversion gain of λ_c=2.5 μm HgCdTe Hawaii-2RG array obtained with stochastic methods. Diamonds: integrated autocorrelation function versus signal. Conversion gain is 227.56 e/mV. Triangles: variance versus signal. Conversion gain is 251.34 e/mV.

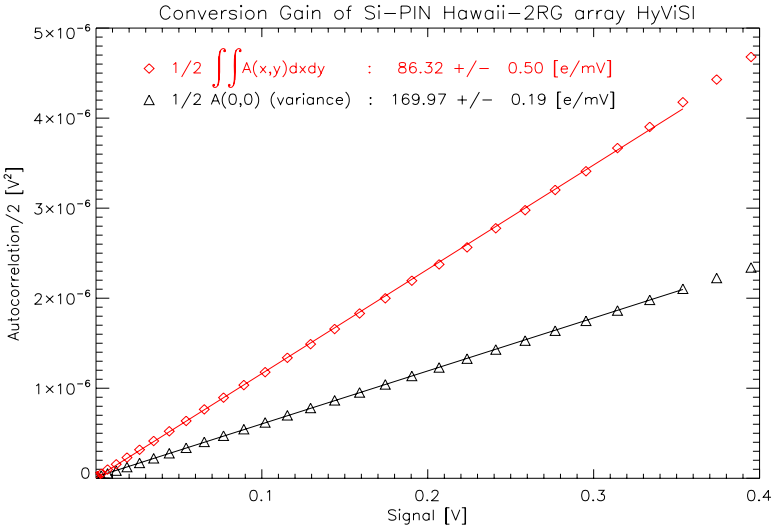

Figure 15 Conversion gain of Si-PIN Hawaii-2RG HyViSI array obtained with stochastic methods. Diamonds: integrated autocorrelation function versus signal. Conversion gain is 86.32 e/mV. Triangles: variance versus signal. Conversion gain is 169.97 e/mV.

7. CONCLUSIONS

The demand for extremely large focal planes on modern telescopes has driven the array format to 2Kx2K, a limit which cannot be surpassed easily because of limited substrate sizes. The only way to increase the format of modern CMOS hybrid arrays to 4Kx4K and beyond is to revert to smaller pixels in the range of 10 – 15 μm. This leads to other limitations such as the coupling capacitances between neighboring pixels which become more important for smaller pixels. Even if the interpixel capacitance is only a few percent of the nodal capacitance of a detector pixel, the coupling

capacitance has to be taken into account to obtain the correct conversion gain with stochastic methods. The usual "noise squared versus signal" method leads to an overestimation of the nodal capacitance of >15% for infrared arrays and 100% for Si-PIN diode arrays. An alternative method of measuring the nodal capacitance, the capacitance comparison technique, is the most direct method and is also simple to implement. It delivers nodal capacitances which yield plausible quantum efficiencies below 100% for both HgCdTe and Si-PIN hybrids. The capacitance comparison method allows to accurately measure the voltage dependence of the nodal capacitance and to derive the doping concentration and the built in voltage of the pn junction in the detector pixel. Also the gate capacitance of the unit cell source follower can be retrieved with this method. Hence all parameters of the detector can be determined experimentally to accurately model the detector response and the linearity. The measured gate capacitance accounts for 65 % of the nodal capacitance and can be reduced in future multiplexer designs in order to reduce the readout noise.

The guide mode of the Hawaii-2RG array makes it possible to apply a single pixel reset and directly measure the impulse response or the point spread function generated by capacitive coupling between adjacent pixels. With this technique a coupling capacitance smaller than 1fF can be easily measured. Contrary to optical crosstalk and charge diffusion, which also contribute to interpixel crosstalk, capacitive coupling between detector pixels is a deterministic process and conserves photometry. The PSF caused by this effect, which can be measured with the single pixel reset method on Hawaii-2RG arrays, can directly be used to deconvolve images. The interpixel capacitance does not depend on the applied bias voltage.

Interpixel coupling can be considered as a process, which attenuates high spatial frequencies similar to an imperfect optical system. The transfer function of this filter is the Fourier transform of the impulse response measured by the single pixel reset method. For point sources the spreading of the signal response to neighboring pixels seriously affects the signal to noise ratio and degrades the detector MTF and image sharpness. When deriving the conversion from noise measurements, the variance has to be replaced by the integrated autocorrelation as an estimator for the photon shot noise. It has been demonstrated that within the experimental uncertainty the capacitance comparison method, the Fe^{55}- method and the integrated 2D autocorrelation deliver the same conversion gain.

The depletion regions of infrared diode arrays are separated by the conducting HgCdTe bulk. Therefore, capacitive coupling can only occur between the In bumps in the space between the infrared array and the Si multiplexer or in the multiplexer itself. Smaller In bumps and a filling epoxy, between the multiplexer and the detector array, having a low dielectric constant help to minimize the coupling. The Si-PIN diode array which we investigated is hybridized to the same Hawaii-2RG multiplexer as the HgCdTe infrared array, but has a much larger interpixel coupling capacitance. Hence, the main contribution to the interpixel capacitance must be located in the fully depleted Si-PIN diode array itself. Optical PSF measurements carried out on a Si-PIN array by Dorn et al [2] confirm, that capacitive coupling between neighboring pixels is the dominant contribution to the detector PSF. It will be a challenge to substantially reduce interpixel coupling in large format arrays with smaller pixel sizes.

REFERENCES

1. G. Finger J. Beletic, R.Dorn, L. Mehrgan, M. Meyer, A. Moorwood, J. Stegmeier, "Conversion gain and interpixel capacitance of CMOS hybrid focal plane arrays", Scientific Detectors for Astronomy 2005, pp. 477-490, June 2005.
2. R. Dorn, S. Eschbaumer, G. Finger, L. Mehrgan, M. Meyer, J. Stegmeier, "A CMOS Visible Silicon Imager hybridized to a Rockwell 2RG multiplexer as a new detector for ground based astronomy**"**, Proc. SPIE 6276, to be published, 2006.
3. J. R. Janesik, Scientific Charge-Coupled Devices, SPIE Press, p. 134, 2001.
4. G. Finger, J. Garnett, N. Bezawada, R. Dorn, L. Mehrgan, M. Meyer, A. Moorwood, J. Stegmeier, G. Woodhouse, "Performance evaluation and calibration issus of large format hybrid active pixel sensors used for ground and space based astronomy", Nuclear Inst. and Methods in Physics Research A, to be published, 2005
5. G. Finger, "PSF of interpixel capacitance", http://www.eso.org/~gfinger/psf_mct.fits, http://www.eso.org/~gfinger/psf_hyvisi.fits, 2006.
6. A. Moore, Z. Ninkov, B. Forrest, "QE Overestimation and Deterministic Crosstalk Resulting from Inter-pixel Capacitance", Optical Engineering, to be published.